Published in final edited form as:

J Immunol. 2015 April 1; 194(7): 3369–3380. doi:10.4049/jimmunol.1402098.

The NLRP1 Inflammasome Attenuates Colitis and Colitis-Associated Tumorigenesis[1]

Tere M. Williams[*], **Rachel A. Leeth**[*], **Daniel E. Rothschild**[*], **Sheryl L. Coutermarsh-Ott**[*], **Dylan K. McDaniel**[*], **Alysha E. Simmons**[*], **Bettina Heid**[*], **Thomas E. Cecere**[*], and **Irving C. Allen**[*,2]

[*]Department of Biomedical Sciences and Pathobiology, Virginia Maryland College of Veterinary Medicine, Virginia Tech, Blacksburg, VA, 24061, USA

Abstract

NLR proteins are a diverse family of pattern recognition receptors that are essential mediators of inflammation and host defense in the gastrointestinal system. Recent studies have identified a sub-group of inflammasome forming NLRs that modulate the mucosal immune response during inflammatory bowel disease (IBD) and colitis associated tumorigenesis. To better elucidate the contribution of NLR family members in IBD and cancer, we conducted a retrospective analysis of gene expression metadata from human patients. These data revealed that NLRP1, an inflammasome forming NLR, was significantly dysregulated in IBD and colon cancer. To better characterize the function of NLRP1 in disease pathogenesis, we utilized *Nlrp1b*$^{-/-}$ mice in colitis and colitis associated cancer models. Here, we report that NLRP1 attenuates gastrointestinal inflammation and tumorigenesis. *Nlrp1b*$^{-/-}$ mice demonstrated significant increases in morbidity, inflammation and tumorigenesis compared to wild type animals. Similar to data previously reported for related inflammsome forming NLRs, the increased inflammation and tumor burden was correlated with attenuated levels of IL-1β and IL-18. Further mechanistic studies utilizing bone marrow reconstitution experiments revealed that the increased disease pathogenesis in the *Nlrp1b*$^{-/-}$ mice was associated with non-hematopoietic derived cells and suggests that NLRP1 functions in the colon epithelial cell compartment to attenuate tumorigenesis. Together, these data identify NLRP1 as an essential mediator of the host immune response during IBD and cancer. These findings are consistent with a model whereby multiple NLR inflammasomes attenuate disease pathobiology through modulating IL-1β and IL-18 levels in the colon.

Keywords

Colon; Cancer; Nod-like receptor; IBD; IL-1β; IL-18; inflammatory bowel disease; NLR; NLRP3; NLRP6; NLRC4

[1]This work was supported by National Institute of Diabetes and Digestive and Kidney Diseases under award K01DK092355 (ICA). The content is solely the responsibility of the authors and does not necessarily represent the official views of the NIH. The authors declare they have no conflict of interest.

[2]Correspondence: Dr. Irving Coy Allen, Virginia Tech, Virginia Maryland College of Veterinary Medicine, Department of Biomedical Sciences and Pathobiology, Blacksburg, VA, 24061, Fax: 1-540-231-7425, USA icallen@vt.edu, Phone: 1-540-231-7551.

INTRODUCTION

Pattern recognition receptors (PRRs) modulate mucosal inflammation in the gut through maintaining a balanced immune response to commensal flora and damage to the epithelial cell barrier (1). Members of the nucleotide-binding domain and leucine-rich repeat containing (NLR) family of PRRs have recently emerged as significant modulators of IBD and cancer pathogenesis (2,3). In human populations, single nucleotide polymorphisms (SNPs) have been identified in a variety of NLRs, including NOD1, NOD2 and NLRP3 that are associated with a genetic predisposition to IBD. Likewise, recent animal studies have characterized several NLRs that are critical modulators of gastrointestinal inflammation and colitis associated cancer (4–8). However, of the 23 human NLR and NLR-like proteins, only about half have been adequately characterized and the clinical relevance of the majority of NLR family members in IBD is unknown (9–11).

The bulk of recent studies have focused on a sub-group of NLRs that function in inflammasome formation. Inflammasomes are macromolecular scaffolds that are composed of an NLR, the adaptor protein ASC, and caspase-1, which form in the cytosol following NLR activation in response to specific microbe- and/or damage-associated molecular patterns (MAMPs and DAMPs) (12). NLR inflammasomes are responsible for the activation of caspase-1 and the subsequent cleavage and maturation of pro-IL-1β and pro-IL-18 into their mature, bioactive cytokines. Prior animal studies utilizing *Asc*$^{-/-}$ and *Casp1/11*$^{-/-}$ mice have demonstrated that loss of either essential inflammasome associated protein results in severe experimental colitis and colitis associated tumorigenesis in common chemical induced models (4,5,7,8,13–16). Due to the robust effects of ASC and Caspase-1 on IBD pathogenesis, it is critical to identify and characterize the specific inflammasome-forming NLRs associated with mucosal immune system homeostasis in the gut.

Of the inflammasome forming NLRs, NLRP1 is a highly interesting candidate to explore in the context of IBD. In human populations, mutations in *NLRP1* have been linked to a variety of diseases associated with dysfunctional immunoregulation, including celiac disease, vitiligo, and type I diabetes (17–20). In the context of IBD, genome wide association studies (GWAS) have identified *NLRP1* mutations that are associated with Crohn's Disease (CD) and in particular were associated with extra-intestinal co-occurring inflammatory manifestations (21). NLRP1 polymorphisms were also found to be associated with IBD steroid responsiveness in a pediatric study (22). The NLRP1 inflammasome was the first inflammasome characterized *in vitro*, but has yet to be sufficiently characterized *in vivo*. NLRP1 is activated by muramyl dipeptide (MDP) in humans and is activated by *Bacillus anthracis* Lethal Toxin (LeTx) and *Toxoplasma gondii* in rodents (23–28). There are multiple species-specific and structurally diverse orthologs of *NLRP1*. For example, rodents have multiple paralogs of the *Nlrp1* gene, including 3 in mice that are poorly characterized (24). The NLRP1a paralog in mice has been shown to regulate homeostatic hematopoiesis and the NLRP1b paralog is associated with LeTx sensitivity (24,25,29,30).

NLRP1 has not been directly evaluated in mouse models of IBD or cancer. Recently, two independent mouse lines lacking NLRP1 (*Nlrp1abc*$^{-/-}$ and *Nlrp1b*$^{-/-}$) have been described (25,29). Both mouse lines were found to be susceptible to *T. gondii* infection and develop

attenuated acute lung injury following LeTx exposure (25,29,31). While exposure to either *T. gondii* or LeTx are unlikely mediators of IBD pathogenesis, further characterization of NLRP1 will likely identify a range of additional MAMPs and DAMPs of greater relevance to gastrointestinal inflammation and cancer. In this study, we evaluate the hypothesis that NLRP1 attenuates the progression of colitis and colitis associated tumorigenesis. Specifically, we utilized *Nlrp1b*$^{-/-}$ mice in models of experimental colitis using dextran sulfate sodium (DSS) and azoxymethane (AOM)/DSS mediated inflammation driven tumorigenesis. This study is the first to functionally evaluate the NLRP1 inflammasome in IBD and demonstrates that NLRP1 is a robust modulator of colitis pathobiology and colitis associated cancer progression.

MATERIALS AND METHODS

Experimental Animals

The generation and characterization of *Nlrp1b*$^{-/-}$ and *Asc*$^{-/-}$ mice has been previously described (25,32). All experiments were conducted with 8–10 week old male mice, unless otherwise noted, that were backcrossed onto the C57Bl/6 background. All studies were controlled with either littermate and/or cohoused wild type animals that were maintained under SPF conditions and received 5010 chow (LabDiet) and water *ad libitum*. All experiments were conducted in accordance with the NIH Guide for the Care and Use of Laboratory Animals and were conducted under institutional IACUC approval.

Induction and Assessment of Experimental Colitis and Colitis Associated Tumorigenesis

Experimental colitis was induced using a single cycle of either 2.5% or 5% DSS (MP Biomedicals) for 4–5 days and the mice were evaluated for up 10 days (33). To evaluate the effects of antibiotics on colitis progression, mice were given water (pH~3) containing ampicillin (1mg/ml), streptomycin (5mg/ml) and vancomycin (0.25mg/ml) daily for two weeks prior to DSS exposure and maintained on this regime throughout the experimental colitis study. For cohousing experiments, age and gender matched wild type and *Nlrp1b*$^{-/-}$ mice were weaned and housed in a 1:1 ratio for 8 weeks prior to DSS exposure. For cytokine reconstitution studies, mice were given daily i.p. injections with either 0.25 μg/g of recombinant mouse IL-18 (Life Technologies) or 10 μg/g of recombinant mouse IL-1β (Sigma). Relapsing/remitting experimental colitis was induced with 3 cycles of 2.5% DSS for 5 days, with 14 day intervals between each cycle (33). Mice were evaluated 10–14 days following the last cycle of DSS. To induce inflammation driven tumorigenesis in the colitis associated cancer model, mice were given one i.p. injection of 10 mg/kg body weight azoxymethane (AOM) (Sigma Aldrich) and subjected to the relapsing/remitting experimental colitis model utilizing 2.5% DSS (34). Mice were euthanized and disease pathogenesis evaluated at specific time points in each model or when moribund. Morbidity and mortality evaluations included assessments of body weight, the presence of blood around the rectum or in the stool and stool consistency. Each of these parameters were scored (scale of 0 – 4) and averaged to generate a cumulative semi-quantitative clinical score, as previously described (4,35). For all animals, whole blood was collected by cardiac puncture and serum isolated under sterile conditions. Endotoxin levels in the serum were

quantified using the Limulus Amebocyte Lysate (LAL) assay (Pierce) following the manufacturer's instructions for serum.

Macroscopic Polyp Analysis and Histopathology Evaluation

Colons were harvested from the cecum to the rectum and flushed with 1X PBS containing penicillin/streptomycin. Each colon was opened longitudinally and macroscopic polyps were identified under 10X magnification. Size was calculated by taking multiple measurements across the maximum surface of each macroscopic polyp (4,35). The colons were subsequently rolled and fixed in 10% buffered formalin for paraffin embedding. Paraffin embedded tissues were sectioned at 5μm and hematoxylin and eosin (H&E) stained. H&E stained sections were evaluated by an experienced investigator (I.C.A.) and/or a board certified veterinary pathologist (T.E.C. or S.L.C.), who was blinded to genotype and treatment. Each section was scored (scale of 0–4) for inflammation, epithelial defects, crypt atrophy, hyperplasia, dysplasia/neoplasia and area affected by disease, as previously detailed (4,35,36). The score for each parameter in the distal and mid colon was summed to generate the Histological Activity Index (HAI) score. Goblet cell hyperplasia and mucus in the colon was evaluated on 5μm sectioned paraffin embedded colon tissues, which were stained using the Alcian-blue/periodic acid-schiff reaction (AB/PAS) (37). Briefly, 2 mm sections of the colon located approximately 1 cm proximal from the termination of the rectum was identified and digitally imaged in an effort to consistently observe similar regions across all colon samples and experiments. The length and area of the AB/PAS stained regions of the epithelium were assessed utilizing ImageJ software (NIH, Springfield, VA), and data are expressed as the mean volume density (Vs) (38). Cell death was evaluated on colon tissues using TUNEL staining (EMD Millipore). Computer assisted image analysis with ImageJ software was also used to evaluate TUNEL positive cells in each colon section and reported as pixels/field of view under 20X magnification. Three sections per mouse were evaluated for both TUNEL and AB/PAS assessments.

Colon Organ Culture and Cytokine Assessments

Colon cytokine levels were determined utilizing an organ culture system, as previously described (4,35,39). Briefly, bisected colon was cut into 1 cm^2 sections and washed with 1X PBS containing penicillin/streptomycin. Each section was weighed and incubated overnight in 500 μl of RPMI 1640 medium at 37°C in an atmosphere containing 5% CO2. The medium contained penicillin/streptomycin, but no additional supplements. Cell free supernatants were collected following centrifugation and cytokine levels were evaluated by ELISA.

Generation of Chimeric Mice by Bone Marrow Reconstitution

Chimeric mice were generated by bone marrow transplantation following standard protocols (40). Recipient mice were lethally irradiated with 1100 rad (equivalent) utilizing 2 equal doses of X-ray irradiation (Rad Source Technologies, Inc.) with a 6 hour interval and 12 hours later the mice received 5×10^6 bone marrow cells from the femurs of WT and *Nlrp1b*$^{-/-}$ mice. Reciprocal bone marrow reconstitution was preformed, which resulted in the generation of the following 4 groups of experimental mice: wild type→wild type

(WT→WT); *Nlrp1b*$^{-/-}$→*Nlrp1b*$^{-/-}$; *Nlrp1b*$^{-/-}$→WT; and WT→*Nlrp1b*$^{-/-}$. Surviving mice were subjected to the AOM/DSS model, 6 weeks after reconstitution.

Human Metadata Analysis

Human *NLRP1* and mouse *Nlrp1* expression was evaluated using a publically accessible microarray meta-analysis search engine (http://www.nextbio.com/b/search/ba.nb), as previously described (41). The following array data series were analyzed to generate the human patient data: Colon Cancer: GSE10972, GSE31279, GSE33126, GSE21815, GSE41328, GSE37364, GSE4107, and GSE35279; Colitis: GSE11223, GSE13367, and GSE6731.

Statistical Analysis

We utilized GraphPad Prism 5 Statistical software to conduct Analysis Of Variance (ANOVA) followed by either Tukey-Kramer HSD or Newman-Keuls post-test to evaluate statistical significance for multiple comparisons. Single data point comparisons were evaluated by the Student's two-tailed t-test. Group survival was assessed utilizing the Kaplan-Meier test. All data are presented as the mean +/− the standard error of the mean (SEM) and in all cases a p-value of less than 0.05 was considered statistically significant.

RESULTS

NLRP1 Attenuates Acute Gastrointestinal Inflammation during Experimentally Induced Colitis

Previous studies have shown that the NLRP3, NLRP6 and NLRC4 inflammasomes significantly contribute to immune system homeostasis during IBD. The current paradigm suggests that each inflammasome forming NLR functions to attenuate IBD pathogenesis through context-specific and non-redundant mechanisms. Thus, we initially sought to evaluate the gene expression of all of the currently identified inflammasome forming NLRs during IBD using a retrospective metadata analysis of publically available gene expression data. During this screen, we discovered that *NLRP1* expression was significantly altered in several datasets associated with IBD. Data from 3 independent studies revealed that NLRP1 was significantly increased in colon biopsies from patients with active ulcerative colitis compared to biopsies collected from healthy donors (Figure 1A). These data suggest that NLRP1 is either directly or indirectly induced by intestinal inflammation.

We next sought to functionally evaluate NLRP1 utilizing *Nlrp1b*$^{-/-}$ mice (25). These animals were exposed to dextran sulfate sodium (DSS), which is a common model of ulcerative colitis and previously utilized to evaluate other NLR inflammasomes in similar studies. Mice were exposed to acute DSS (5%) for 4–5 days and morbidity and mortality were evaluated for up to 10 days. *Nlrp1b*$^{-/-}$ mice were found to be hypersensitive to the DSS administration and demonstrated a significant decrease in survival, with over half of the animals requiring euthanasia by day 8 (Figure 1B). In the DSS model, weight loss is typically considered to be a surrogate measurement of disease progression. Consistent with the survival data, the *Nlrp1b*$^{-/-}$ mice lost a significant amount of body weight between days 6 and 8 and did not recover at the same rate as the wild type animals (Figure 1C). Hallmark

clinical parameters associated with disease progression were also evaluated and scored. The clinical scores for mock treated *Nlrp1b*$^{-/-}$ mice tended to skew higher than the scores for the mock treated wild type animals (Figure 1D). In this model, the average daily clinical score typically ranges from 0.0 to 0.75, thus the animals are still considered to be within normal limits of the assessment, but trend higher compared to the wild type animals (Figure 1D). DSS administration induced a significant increase in clinical features associated with disease in wild type and *Nlrp1b*$^{-/-}$ mice following DSS administration; however, disease progression was significantly greater in the *Nlrp1b*$^{-/-}$ animals (Figure 1D). Together, these data indicate that NLRP1 plays a protective role during experimental colitis in mice.

Previous studies have revealed that components of the host microbiota significantly contribute to disease pathobiology. For example, the commensal microbiota composition in the *Nlrp6*$^{-/-}$ mice was found to be significantly altered compared to wild type animals and this distorted microbiota was suggested to be directly associated with disease pathogenesis in IBD (6,14). NLRP1 is one of the few NLRs functionally shown to detect both prokaryotic and eukaryotic MAMPs (26,31). Thus, to broadly evaluate the contribution of the bacterial components of the host microbiota to disease pathogenesis in the *Nlrp1b*$^{-/-}$ mice, animals were treated daily with a broad spectrum antibiotic cocktail prior to and throughout exposure to DSS. Antibiotic ablation significantly reversed the sensitivity of both wild type and *Nlrp1b*$^{-/-}$ mice to DSS (Figure 1E; Supplemental Figure 1A–B). While the antibiotic ablation studies are broad, these data indicate a robust contribution of the bacterial components of the host microbiota in driving experimental colitis pathogenesis in the *Nlrp1b*$^{-/-}$ mice.

Prior studies have shown that DSS sensitivity is transmissible from *Asc*$^{-/-}$ and *Nlrp6*$^{-/-}$ animals to wild type mice due to significant alterations in the composition of the fecal microbiota (16,42). To further evaluate the contribution of the microbiota and transmissibility of DSS hypersensitivity, we weaned and cohoused *Nlrp1b*$^{-/-}$ mice with age-matched wild type animals for 8 weeks prior to DSS exposure. Similar to the previous findings reported for *Asc*$^{-/-}$ and *Nlrp6*$^{-/-}$ mice, co-housing wild type animals with *Nlrp1b*$^{-/-}$ mice resulted in the development of severe experimental colitis pathogenesis in the wild type mice. Wild type animals demonstrated a significant increase in weight loss and morbidity, which was comparable to the levels observed in the *Nlrp1b*$^{-/-}$ mice (Figure 1F). Together, the findings from the antibiotic ablation and co-housing studies suggest that the phenotype associated with the *Nlrp1b*$^{-/-}$ mice is transmissible and further implicates alterations of the host microbiota in facilitating DSS hypersensitity in these animals.

Acute distal colon inflammation and damage to the epithelial cell barrier are hallmark pathological characteristics associated with the experimental colitis model. All of the DSS treated mice demonstrated increases in both of these parameters (Figure 2A–D). However, *Nlrp1b*$^{-/-}$ mice developed histological features associated with disease progression that were increased compared to the wild type animals (Figure 2A). Previous studies have shown that mice lacking the inflammasome adaptor protein ASC develop severe colitis, which is significantly increased compared to *Nlrp3*$^{-/-}$, *Nlrc4*$^{-/-}$ and *Nlrp6*$^{-/-}$ mice. Consistent with these previous findings, *Asc*$^{-/-}$ mice utilized in the current study were more hypersensitive to DSS compared to the *Nlrp1b*$^{-/-}$ mice and presented with augmented histopathological

features associated with disease progression (Figure 2A). In the experimental colitis model, the Histological Activity Index (HAI) score provides a semi-quantitative assessment of colon histopathology (36). All of the mice exposed to DSS demonstrated a significant increase in HAI compared to the mock-treated animals. However, HAI assessments revealed that the *Nlrp1b*$^{-/-}$ mice developed intermediate disease that was significantly increased compared to the wild type animals and significantly attenuated compared to the *Asc*$^{-/-}$ mice (Figure 2B). Further evaluation of the components of the HAI score revealed that distal colon inflammation and epithelial cell defects were the greatest contributors to the increased histopathology observed in the *Nlrp1b*$^{-/-}$ animals, whereas all of the individual scores in the mid and distal colon were significantly increased in the more severe *Asc*$^{-/-}$ mice (Figure 2B; Supplemental Figure 2A–F). In addition to histopathology assessments, we also evaluated the level of serum endotoxin following DSS exposure. Previous studies have correlated the level of serum endotoxin with epithelial barrier dysfunction in the experimental colitis model (43). Following DSS administration, serum endotoxin levels were significantly increased in all mice following DSS administration (Supplemental Figure 2G). Consistent with the increased epithelial barrier damage in the *Asc*$^{-/-}$ and *Nlrp1b*$^{-/-}$ animals, we routinely observed increased levels of serum endotoxin in these mice compared to wild type animals; however, these data did not reach statistical significance due to high variability in the inflammasome deficient mice (Supplemental Figure 2G). Together, these data identify the NLRP1 inflammasome as an essential mediator of inflammation in the gut and significantly contributes to mucosal immune system homeostasis during colitis.

Colitis Sensitivity in the *Nlrp1b*$^{-/-}$ Mice is Correlated with IL-1β and IL-18 Attenuation

NLR inflammasome formation results in the cleavage of pro-IL-1β and pro-IL-18, which results in the maturation of these cytokines into their bioactive states. Prior studies evaluating ASC and Caspase-1 in similar models of ulcerative colitis have revealed that the levels of these cytokines are commonly found to be ablated in *Asc*$^{-/-}$ and *Casp1*$^{-/-}$/*11*$^{-/-}$ mice (4–6,8). Likewise, IL-1β and IL-18 levels are also attenuated in the absence of NLRP3, NLRC4 and NLRP6 in the DSS model (4,6–8). To evaluate local cytokine levels in the colon, we generated organ cultures following necropsy (4,35). Following overnight incubation, the colon supernatants were collected and protein levels were assessed by ELISA. DSS treatment increased IL-1β, IL-18 and IL-6 in all of the animals compared to levels observed in the mock treated mice (Figure 3A–C). However, IL-1β and IL-18 levels in the supernatants collected from the *Nlrp1b*$^{-/-}$ animals were significantly reduced compared to the wild type mice (Figure 3A–B). The levels of IL-6 between the DSS treated wild type and *Nlrp1b*$^{-/-}$ animals were not significantly altered (Figure 3C).

The contribution of IL-1β and IL-18 during IBD is currently unclear and in many cases contradictory. Previous studies have shown that attenuated levels of both of these cytokines are typically observed in the absence of NLR inflammasomes and are correlated with enhanced disease pathogenesis in the experimental colitis and colitis associated tumorigenesis models (4–6,8,16). To directly evaluate the contribution of each of these cytokines, *Nlrp1b*$^{-/-}$ mice were reconstituted with either recombinant mouse IL-1β or IL-18 during DSS exposure. The *Nlrp1b*$^{-/-}$ mice that received IL-18 demonstrated significantly reduced weight loss and attenuated disease pathogenesis compared to the saline treated

animals (Figure 3D–E). Likewise, we also observed a significant attenuation in disease pathogenesis in the *Nlrp1b*$^{-/-}$ mice that were treated with IL-1β (Figure 3D–E). Previous studies have shown that attenuated levels of IL-18 are associated with diminished epithelial barrier function, which increases colitis severity in other NLR inflammasome deficient mouse strains (13). While these data are consistent with these prior studies, our findings also suggest that IL-1β plays an important role in attenuating disease pathogenesis in the *Nlrp1b*$^{-/-}$ mice.

NLRP1 Contributes to Attenuation of Tumorigenesis during Colorectal Carcinoma and Colitis Associated Tumorigenesis

We next sought to evaluate the contribution of NLRP1 in the development of intestinal malignancies and colitis associated colorectal carcinoma (CRC). To evaluate the possibility that NLRP1 may contribute to colorectal cancer pathogenesis, we conducted a retrospective evaluation of publically available gene expression metadata compiled from 8 independent studies that evaluated colon biopsies from areas of cancer versus adjacent tissue or biopsies/tissue from colon cancer patients compared with healthy controls (Figure 4A). NLR gene expression from each study was averaged and revealed that NLRP1 was significantly down-regulated in all of the evaluated datasets (Figure 4A). In addition to NLRP1, we also evaluated the other 3 NLRs previously reported to modulate tumorigenesis in the colon. While none of the NLRs were dysregulated in studies comparing colon cancer to adjacent tissue, NLRP3 and NLRC4 were found to be significantly up-regulated in cancer biopsies compared to healthy or normal patients, whereas NLRP6 expression was unchanged in all studies (Figure 4A). Together, these data indicate that NLRP1 is down-regulated in the context of tumorigenesis in human patient populations, whereas NLRP3 and NLRC4 are directly induced or up-regulated, likely as part of a feedback response during disease progression. Likewise, these data underscore the value of additional mechanistic studies to better determine the function of these NLRs in patient populations.

To gain additional insight into the role of the NLRP1inflammasome in the development and progression of CAC, we utilized the AOM/DSS model of inflammation driven colon tumorigenesis. AOM is a mutagen that exerts mild colonotropic carcinogenicity when administered by itself; however, this process is greatly enhanced by combining with DSS in a model of relapsing remitting colitis. The *Nlrp1b*$^{-/-}$ mice have been thoroughly evaluated by our lab and others and no overt spontaneous inflammation or cancer phenotypes have been observed. Thus, to induce tumorigenesis in these animals, the *Nlrp1b*$^{-/-}$ mice were treated with a single dose of AOM followed by 3 rounds of 2.5% DSS over the course of 2 months. By day 60, 16% of the *Nlrp1b*$^{-/-}$ mice had progressed to the point of requiring euthanasia, which was statistically significant compared to 3% of the wild type animals (Figure 4B). Further assessments of weight change throughout the course of the colitis driven tumorigenesis model revealed that the *Nlrp1b*$^{-/-}$ mice are hypersensitive to the lower dosages of DSS and show significant weight loss during the early stages of the model compared to the wild type animals (Figure 4C; Supplemental Figure 3A). Following each DSS administration, the mice recover; however the recovery never fully reaches the levels observed for the wild type animals until the final DSS administration (Figure 4C). The *Nlrp1b*$^{-/-}$ mice were also found to be hypersensitive to DSS administration alone; however,

the weight changes were not as robust compared to the AOM/DSS treated animals (Supplemental Figure 3A). No significant differences in disease progression were noted between the wild type and *Nlrp1b*$^{-/-}$ AOM only or mock treated animals (Supplemental Figure 3A–B). These clinical findings suggest that NLRP1 is necessary for alleviating mouse morbidity and mortality during inflammation driven colon tumorigenesis. Furthermore, when combined with the findings that *NLRP1* is down-regulated in human patients during colon cancer, these data suggest that NLRP1 functions as a critical modulator of colon homeostasis during tumorigenesis.

Prior studies have revealed NLR inflammasome activity attenuates colitis associated cancer. Specifically, *Asc*$^{-/-}$ and *Casp1*$^{-/-}$/*11*$^{-/-}$ mice develop severe gastrointestinal inflammation and colon tumorigenesis in AOM/DSS models (4,5,8). Because ASC and Caspase-1 are shared components of all NLR inflammasomes, we sought to specifically assess the contribution of NLRP1 in the CAC model. Upon completion of the AOM/DSS challenge (Day 64), colons were removed and macroscopic polyps were evaluated. Polyps were detected in all of the AOM/DSS treated mice (Figure 5A). However, we observed a significant increase in the average number of polyps in the *Nlrp1b*$^{-/-}$ (2.57 ± 0.75) and *Asc*$^{-/-}$ animals (4.25 ± 1.33) compared to the wild type mice (0.75 ± 0.23)(Figure 5A). In addition to being more numerous, the polyps in the *Nlrp1b*$^{-/-}$ (10.60 mm^2 ± 1.78) and *Asc*$^{-/-}$ mice (7.97 mm^2 ± 1.46) were also significantly larger than those observed in the wild type animals (2.34 mm^2 ± 0.44) (Figure 5B). Histopathology assessments revealed increased inflammation, hyperplasia and dysplasia in the *Nlrp1b*$^{-/-}$ and *Asc*$^{-/-}$ mice (Figure 5C). HAI assessments revealed a significant increase in colon histopathology in all of the DSS and AOM/DSS treated animals, compared to the mock and AOM only treated mice (Figure 5D). However, consistent with the increase in macroscopic polyps, AOM/DSS treated *Nlrp1b*$^{-/-}$ and *Asc*$^{-/-}$ mice had significantly greater HAI scores compared to wild type animals (Figure 5D). Further assessments of the parameters that compose the HAI score revealed significant increases in colon hyperplasia and dysplasia was a major contributor to the higher composite scores observed in these mice (Figure 5E–F; Supplemental Figure 3C–J). Typically, AOM/DSS administration results in disease pathogenesis that is restrained to the distal colon. However, in both *Nlrp1b*$^{-/-}$ and *Asc*$^{-/-}$ animals, extensive histopathology was observed to extend into the mid and proximal colon, which was also a contributing factor associated with the higher composite scores (Supplemental Figure 3C–J). In addition to histopathological assessments of inflammation and tumorigenesis, we also conducted basic assessments of epithelial cell death in the *Nlrp1b*$^{-/-}$ mice. Here, we utilized TUNEL staining of colon sections following relapsing remitting experimental colitis and colitis associated tumorigenesis. TUNEL stained colon sections were imaged and digitally analyzed to generate a semi-quantitative assessment of epithelial cell death. Following DSS exposure, we observed significantly increased TUNEL positive cells in the *Nlrp1b*$^{-/-}$ mice compared to wild type animals (Figure 5G). Likewise, *Nlrp1b*$^{-/-}$ mice also demonstrated increased cell death in the context of colitis associated tumorigenesis compared to the wild type animals (Figure 5G). Consistent with the increased cell death and epithelial barrier dysfunction, we also observed increased levels of endotoxin in serum collected from *Nrlp1b*$^{-/-}$ animals compared to wild type mice (Supplemental Figure 3K). Serum endotoxin levels were routinely higher in the *Nlrp1b*$^{-/-}$ and *Asc*$^{-/-}$ mice

compared to wild type, but did not reach statistical significance due to high, but variable levels detected in the *Nlrp1b*$^{-/-}$ and *Asc*$^{-/-}$ animals (Supplemental Figure 3K).

Enhanced Tumorigenesis in the *Nlrp1b*$^{-/-}$ Mice is correlated with Attenuated Levels of IL-1β and IL-18

Previous studies evaluating NLR inflammasome signaling during colitis associated cancer revealed that both relapsing remitting colitis progression and colitis associated tumorigenesis were correlated with attenuation of IL-1β and IL-18. Indeed, similar to the findings reported in the experimental colitis models, *Asc*$^{-/-}$ and *Casp1*$^{-/-}$/*11*$^{-/-}$ mice typically demonstrate ablation of these cytokines (4,5,8,14). To assess this mechanism in the *Nlrp1b*$^{-/-}$ mice, we evaluated these and other inflammatory mediators in the organ culture supernatants following completion of the CAC model. We observed a significant increase in all of the cytokines evaluated in colons collected from the wild type mice compared to mock treated animals (Figure 6A–D). However, IL-1β and IL-18 levels were significantly attenuated following AOM/DSS treatment in the *Nlrp1b*$^{-/-}$ colon supernatant compared to the wild type samples (Figure 6A–B). Likewise, IL-1β was significantly attenuated and IL-18 was completely ablated in colons harvested from *Asc*$^{-/-}$ mice compared to the wild type animals (Figure 6A–B). In addition to IL-1β and IL-18, IL-6 levels have also been routinely reported to be increased in NLR inflammasome deficient mice (4). Consistent with these previous observations, IL-6 was significantly increased in the *Nlrp1b*$^{-/-}$ and *Asc*$^{-/-}$ colons compared to wild type (Figure 6C). The increased IL-6 is presumably associated with the heightened disease state in these animals, rather than directly associated with NLR inflammasome function. The immunomodulatory cytokine IL-10 is an essential regulator of gastrointestinal inflammation in the gut and *Il-10*$^{-/-}$ mice develop spontaneous colitis and are prone to developing adenocarcinoma. Thus, we also evaluated IL-10 levels and found that this cytokine was significantly increased in all of the animal groups, with no differences between genotypes (Figure 6D). Together, these data support our hypothesis that the increased colitis associated tumorigenesis in the *Nlrp1b*$^{-/-}$ mice is associated with attenuated levels of IL-1β and IL-18 in the colon.

In addition to modulating IL-1β and IL-18, recent studies evaluating the mechanism associated with NLRP6 inflammasome attenuation of colitis associated tumorigenesis have shown an increased correlation between disease severity and attenuated mucus production in the *Nlrp6*$^{-/-}$ and *Asc*$^{-/-}$ mice (14,42). To assess this mechanism in the context of NLRP1 inflammasome deficiency, we evaluated goblet cell hyperplasia in the colon using Alcian-blue/periodic acid-schiff (AB/PAS) staining (Figure 6E). All of the mice exposed to AOM/DSS demonstrated increased goblet cell hyperplasia compared to the mock treated animals, with no differences observed between wild type, *Asc*$^{-/-}$ and *Nlrp1b*$^{-/-}$ mice (Figure 6E). To better characterize these observations, we utilized a semi-quantitative scoring system, previously proven to be effective in evaluating goblet cell hyperplasia and mucus production in the lungs, to quantify mucus production in the colon (37,38). Consistent with the histopathology assessments, all of the AOM/DSS treated mice demonstrated significantly increased goblet cell hyperplasia compared to the mock treated animals, with no significant differences observed between genotypes (Figure 6F). Thus, NLRP1 does not appear to affect mucus production in the gut during the inflammation

driven tumorigenesis model, and appears to function through a mechanism with characteristics that are distinct from those described for NLRP6.

NLRP1 Attenuates Colitis Associated Tumorigenesis through Non-Hematopoietic Derived Cells

NLR family members have been shown to significantly influence the progression of gastrointestinal inflammation and tumorigenesis through both epithelial cells and hematopoietic derived cells (4,6,8,16). To evaluate cell types of potential relevance to NLRP1 function, we evaluated the expression of 25 NLR and NLR associated genes in human colon epithelial cells and monocytes. In general, all of the NLRs were found to be expressed in both cell types (Supplemental Figure 4A–B). However, NLRP1 was the only inflammasome forming NLR to be highly up-regulated in epithelial cells (Supplemental Figure 4A–B). Thus, to better evaluate the mechanism underlying NLRP1 function, we generated wild type and *Nlrp1b*$^{-/-}$ chimeric mice via adoptive bone marrow transplantation (4,35). Mice were lethally irradiated and the reciprocal bone marrow transplants were conducted, as shown in Figure 7A. Following 6 weeks of reconstitution, near-complete chimerism was achieved and the animals were evaluated in the AOM/DSS model. It should be noted that all of the chimera studies were conducted on female mice. Due to the long term nature of these studies, female mice tend to be less aggressive; however, in our hands they also have attenuated responses in the AOM/DSS model. All of the animals experienced weight loss following the first DSS administration. However, all of the *Nlrp1b*$^{-/-}$ chimeric mice failed to gain significant weight compared to the 16.63 ± 2.04% gain observed in the wild type → wild type (WT→WT) mice (Figure 7B). As the model progressed, we observed increased clinical features associated with disease pathogenesis in the WT→*Nlrp1b*$^{-/-}$ and *Nlrp1b*$^{-/-}$→*Nlrp1b*$^{-/-}$ animals. These two groups of mice demonstrated significant increases in their clinical scores compared to the WT→WT and *Nlrp1b*$^{-/-}$→WT mice (Figure 7C). Mice were necropsied on Day 61 and the colon length was evaluated. Colon length is a surrogate evaluation for disease pathogenesis in the AOM/DSS model. Consistent with the clinical score findings, we observed a significant decrease in colon length in the *Nlrp1b*$^{-/-}$→*Nlrp1b*$^{-/-}$ animals and an intermediate difference in colon length for the WT→*Nlrp1b*$^{-/-}$ mice (Figure 7D). Evaluation of macroscopic polyps revealed a significant increase in the number of polyps observed in the *Nlrp1b*$^{-/-}$→*Nlrp1b*$^{-/-}$ and WT→*Nlrp1b*$^{-/-}$ mice, with no polyps detected in the WT→WT or *Nlrp1b*$^{-/-}$→WT animals (Figure 7E). Similar to our previous observations in the non-chimeric animals, many of these polyps were detected in the proximal colon as opposed to the distal regions. Further evaluation of histopathology revealed that WT→*Nlrp1b*$^{-/-}$ and *Nlrp1b*$^{-/-}$→*Nlrp1b*$^{-/-}$ mice had significantly increased HAI scores compared to the WT→WT mice (Figure 7F). Whereas, no significant difference was observed between the WT→WT and *Nlrp1b*$^{-/-}$→WT animals (Figure 7F). Further evaluation of the components of the HAI score revealed that increased distal and proximal inflammation and hyperplasia were the most significant contributors to the higher HAI scores observed in these chimeric mice (Figure 7G–H). Together, these data suggest that NLRP1 functions through the non-hematopoietic compartment, likely intestinal epithelial cells, to attenuate inflammation driven tumorigenesis.

DISCUSSION

NLRs function as sentinel PRRs that sense components of the microbiota and maintain immune system homeostasis in the gut. In human populations, several single nucleotide polymorphisms (SNPs) in NLR genes, including NOD2 and NLRP3, have been associated with genetic predispositions to IBD. However, the spatial and temporal specificities and mechanisms associated with immunoregulation by the NLRs are not adequately characterized in either human or rodent models of disease. In the retrospective metadata analysis shown here, it is clear that NLRP1 is significantly dysregulated in the context of IBD and colon cancer (Figure 1A; Figure 4A). Here, we expand upon these data and show that NLRP1 plays a protective role during experimental colitis and colitis-associated tumorigenesis in the mouse.

The adaptor protein ASC and Caspase-1 exert robust protective effects on IBD and cancer pathogenesis. In the context of inflammasome formation, these proteins interact with a wide range of NLRs. There are 8 NLR and NLR-like proteins that have been strongly characterized as being capable of forming an inflammasome following activation, including NLRP3, NLRC4 and NLRP6. All 3 of these inflammasome forming NLRs have been previously shown to attenuate the progression of IBD and colitis associated cancer (4,6,8,44). In general, the phenotypes observed in the *Nlrp1b*$^{-/-}$ mice are similar to those previously reported for the other NLR deficient mouse lines, including those observed for *Nlrp6*$^{-/-}$ mice and previously by our laboratory for *Nlrp3*$^{-/-}$ animals in these models (4,6,8,16). However, the polyps and tumors in the *Nlrp1b*$^{-/-}$ mice occur much more proximal than those observed in the *Nrlp3*$^{-/-}$ animals and are much larger in size (Figure 5; (4)). Likewise, the phenotypes observed in the *Nlrp1b*$^{-/-}$ mice are also associated with the non-hematopoietic compartment; whereas, the phenotype in the *Nlrp3*$^{-/-}$ animals have been previously associated with the hematopoietic compartment when assessed under similar conditions (Figure 7; (4)). While several studies have suggested that the epithelial cell compartment may be a source of IL-1β and IL-18, our data may also reflect other potential biological functions of NLRP1 in non-hematopoietic derived cells that may include modulation of reactive oxygen species production, cell death or autophagy. Together, these data are consistent with the hypothesis that multiple NLRs function to initiate inflammasome formation and maintain mucosal immune system homeostasis though cell type, temporal and stimuli specific mechanisms that are similar, but non-redundant.

Similar to the findings from other NLR inflammasome studies, IL-1β and IL-18 levels in the *Nlrp1b*$^{-/-}$ colons were significantly decreased. Likewise, our reconstitution studies indicated that both of these cytokines play a protective role in the absence of NLRP1. IL-1β and IL-18 are highly related pro-inflammatory cytokines that are strongly associated with IBD and cancer pathogenesis. Indeed, high levels of IL-1β are often observed in patients with active IBD, where this cytokine functions as a potent stimulator of macrophages, dendritic cells, neutrophils and epithelial cells (45–47). Also, in the context of IBD, IL-1β regulates leukocyte migration into the lamina propria of the intestine and strongly promotes T cell activation, survival, and differentiation (48–52). However, while the role of IL-1β is well characterized in IBD and tumorigenesis, IL-18 has only recently emerged as a primary modulator of mucosal immune system homeostasis. Similar to IL-1β, IL-18 has strong pro-

inflammatory activities and is essential for the proper regulation of CD4+ T cell function and Th1 cell differentiation (53). Likewise, IL-18 levels are commonly dysregulated in human IBD patients and mutations in the *IL-18* gene are associated with UC (54,55). In mice, both IL-18 overexpression and attenuation have been demonstrated to increase pathogenesis in IBD models, which suggest that this cytokine has multiple functions, both positive and negative, during disease progression (6,56–58). This dichotomy between IL-1β and IL-18 in IBD and cancer models can be reconciled by recent findings, which revealed that both IL-1β and IL-18 play essential roles in maintaining the integrity of the epithelial barrier in the colon (6,59). Thus, the current paradigm indicates that NLR inflammasomes exert protective effects in the gut during IBD and inflammation driven tumorigenesis by either directly or indirectly maintaining the function of the epithelial barrier. The findings presented here for IL-1β and IL-18 levels in the *Nlrp1b*$^{-/-}$ mice in both models of colitis and colitis associated tumorigenesis are consistent with this proposed model.

Together, our data strengthens the hypothesis that each NLR functions to attenuate IBD pathogenesis and cancer through context-specific and non-redundant mechanisms. For example, previous studies have indicated that NLRP3 and NLRP6 strongly influence colitis and cancer progression; however, the proposed mechanisms significantly differ. NLRP3 is responsible for sensing a wide range of MAMPs and DAMPs that are associated with damage to the colonic epithelial layer and bacteria translocation following the wound healing response that is initiated by DSS administration. Due to the wide range of stimuli and biological function associated with NLRP3 activation, it is highly probable that this NLR functions through an indirect mechanism to attenuate disease pathogenesis. For example, our previous studies have suggested that IBD and cancer sensitivity in the *Nlrp3*$^{-/-}$ mice is associated with a failure of the hematopoietic cells to properly sense and respond to epithelial cell damage in the DSS and AOM/DSS models (4). However, NLRP6 appears to function more directly through the epithelial cell compartment to modulate IBD and tumor progression (6,14). Recent studies utilizing *Nlrp6*$^{-/-}$ mice have revealed that these animals have a significant expansion of *Bacteroidetes* (Prevotellaceae) that is highly correlated with the severity of IBD pathogenesis (14). The bacteria expansion has been associated with defective goblet cell autophagy and subsequent reductions in mucin granule exocytosis in the *Nlrp6*$^{-/-}$ and *Asc*$^{-/-}$ mice. This appears to allow Prevotellaceae to colonize in the crypts of these animals and establish a persistent infection (42). It is clear that NLRP1 senses a less diverse range of signals compared to NLRP3. NLRP1 has only been shown to sense *B. anthracis* LeTx and *Toxoplasma gondii* in rodents (23–28). These pathogens are not common constituents of the mouse microbiota and are unlikely to be associated with the increased sensitivity of the *Nlrp1b*$^{-/-}$ mice to the induction of colitis and tumorigenesis. Likewise, we also evaluated goblet cell hyperplasia in the *Asc*$^{-/-}$ and *Nlrp1b*$^{-/-}$ mice and did not observe significantly attenuated levels of mucus production in either mouse line. Thus, NLRP1 appears to function through a mechanism that is independent of that recently suggested for NLRP6. With the recent generation of multiple NLRP1 deficient mice, we anticipate that future studies will better define and characterize the *in vivo* stimuli sensed by this unique NLR and provide greater insight underlying the mechanism associated with IBD and cancer.

Over the last decade, significant progress has been made in the identification and characterization of NLR family members. It is becoming increasingly clear that NLRs are essential mediators of the balance that exists in mucosal tissues between the microbiota and the host immune response. However, the clinical relevance and mechanistic details associated with NLR modulation of immunity and therapeutic potential in IBD and cancer is still inadequately understood. Likewise, their contributions to biological functions beyond microbe recognition are relatively unknown in the context of gastrointestinal health and disease. We anticipate that additional studies will reveal and better characterize the microbial elements sensed by NLRP1 in the gut and will provide additional mechanistic insight associated with its role in attenuating disease pathobiology.

Supplementary Material

Refer to Web version on PubMed Central for supplementary material.

Acknowledgments

The authors would like to acknowledge and thank Dr. Beverly H. Koller (UNC Chapel Hill) for the generous supply of *Nlrp1b*$^{-/-}$ mice utilized in this work. We would also like to recognize Dr. Jenny P.-Y. Ting (UNC Chapel Hill) for technical discussions and guidance pertaining to the development of this manuscript. Likewise, we would also like to acknowledge Dr. Christian Jobin (University of Florida) and Dr. Hans Herfarth (UNC Chapel Hill) for technical assistance pertaining to experimental design and macroscopic polyp evaluation assistance. We would also like to recognize the Virginia Tech Post Baccalaureate Research and Education Program (PREP) and the Virginia Tech Initiative for Maximizing Student Development (VT-IMSD) Programs for student support throughout this project.

References

1. Walsh D, McCarthy J, O'Driscoll C, Melgar S. Pattern recognition receptors--molecular orchestrators of inflammation in inflammatory bowel disease. Cytokine & growth factor reviews. 2013; 24:91–104. [PubMed: 23102645]
2. Allen IC. Non-Inflammasome Forming NLRs in Inflammation and Tumorigenesis. Frontiers in immunology. 2014; 5:169. [PubMed: 24795716]
3. Davis BK, Philipson C, Hontecillas R, Eden K, Bassaganya-Riera J, Allen IC. Emerging Significance of NLRs in Inflammatory Bowel Disease. Inflammatory bowel diseases. 2014; 20:2412–2432. [PubMed: 25153506]
4. Allen IC, TeKippe EM, Woodford RM, Uronis JM, Holl EK, Rogers AB, Herfarth HH, Jobin C, Ting JP. The NLRP3 inflammasome functions as a negative regulator of tumorigenesis during colitis-associated cancer. The Journal of experimental medicine. 2010; 207:1045–1056. [PubMed: 20385749]
5. Dupaul-Chicoine J, Yeretssian G, Doiron K, Bergstrom KS, McIntire CR, LeBlanc PM, Meunier C, Turbide C, Gros P, Beauchemin N, Vallance BA, Saleh M. Control of intestinal homeostasis, colitis, and colitis-associated colorectal cancer by the inflammatory caspases. Immunity. 2010; 32:367–378. [PubMed: 20226691]
6. Elinav E, Strowig T, Kau AL, Henao-Mejia J, Thaiss CA, Booth CJ, Peaper DR, Bertin J, Eisenbarth SC, Gordon JI, Flavell RA. NLRP6 inflammasome regulates colonic microbial ecology and risk for colitis. Cell. 2011; 145:745–757. [PubMed: 21565393]
7. Hu B, Elinav E, Huber S, Booth CJ, Strowig T, Jin C, Eisenbarth SC, Flavell RA. Inflammation-induced tumorigenesis in the colon is regulated by caspase-1 and NLRC4. Proceedings of the National Academy of Sciences of the United States of America. 2010; 107:21635–21640. [PubMed: 21118981]

8. Zaki MH, Boyd KL, Vogel P, Kastan MB, Lamkanfi M, Kanneganti TD. The NLRP3 inflammasome protects against loss of epithelial integrity and mortality during experimental colitis. Immunity. 2010; 32:379–391. [PubMed: 20303296]
9. Schroder K, Tschopp J. The inflammasomes. Cell. 2010; 140:821–832. [PubMed: 20303873]
10. Ting JP, Davis BK. CATERPILLER: a novel gene family important in immunity, cell death, and diseases. Annual review of immunology. 2005; 23:387–414.
11. Ting JP, Lovering RC, Alnemri ES, Bertin J, Boss JM, Davis BK, Flavell RA, Girardin SE, Godzik A, Harton JA, Hoffman HM, Hugot JP, Inohara N, Mackenzie A, Maltais LJ, Nunez G, Ogura Y, Otten LA, Philpott D, Reed JC, Reith W, Schreiber S, Steimle V, Ward PA. The NLR gene family: a standard nomenclature. Immunity. 2008; 28:285–287. [PubMed: 18341998]
12. Martinon F, Burns K, Tschopp J. The inflammasome: a molecular platform triggering activation of inflammatory caspases and processing of proIL-beta. Molecular cell. 2002; 10:417–426. [PubMed: 12191486]
13. Zaki MH, Vogel P, Body-Malapel M, Lamkanfi M, Kanneganti TD. IL-18 production downstream of the Nlrp3 inflammasome confers protection against colorectal tumor formation. Journal of immunology. 2010; 185:4912–4920.
14. Hu B, Elinav E, Huber S, Strowig T, Hao L, Hafemann A, Jin C, Wunderlich C, Wunderlich T, Eisenbarth SC, Flavell RA. Microbiota-induced activation of epithelial IL-6 signaling links inflammasome-driven inflammation with transmissible cancer. Proceedings of the National Academy of Sciences of the United States of America. 2013; 110:9862–9867. [PubMed: 23696660]
15. Normand S, Delanoye-Crespin A, Bressenot A, Huot L, Grandjean T, Peyrin-Biroulet L, Lemoine Y, Hot D, Chamaillard M. Nod-like receptor pyrin domain-containing protein 6 (NLRP6) controls epithelial self-renewal and colorectal carcinogenesis upon injury. Proceedings of the National Academy of Sciences of the United States of America. 2011; 108:9601–9606. [PubMed: 21593405]
16. Chen GY, Liu M, Wang F, Bertin J, Nunez G. A functional role for Nlrp6 in intestinal inflammation and tumorigenesis. Journal of immunology. 2011; 186:7187–7194.
17. Jin Y, Birlea SA, Fain PR, Spritz RA. Genetic variations in NALP1 are associated with generalized vitiligo in a Romanian population. The Journal of investigative dermatology. 2007; 127:2558–2562. [PubMed: 17637824]
18. Levandowski CB, Mailloux CM, Ferrara TM, Gowan K, Ben S, Jin Y, McFann KK, Holland PJ, Fain PR, Dinarello CA, Spritz RA. NLRP1 haplotypes associated with vitiligo and autoimmunity increase interleukin-1beta processing via the NLRP1 inflammasome. Proceedings of the National Academy of Sciences of the United States of America. 2013; 110:2952–2956. [PubMed: 23382179]
19. Magitta NF, Boe Wolff AS, Johansson S, Skinningsrud B, Lie BA, Myhr KM, Undlien DE, Joner G, Njolstad PR, Kvien TK, Forre O, Knappskog PM, Husebye ES. A coding polymorphism in NALP1 confers risk for autoimmune Addison's disease and type 1 diabetes. Genes and immunity. 2009; 10:120–124. [PubMed: 18946481]
20. Pontillo A, Vendramin A, Catamo E, Fabris A, Crovella S. The missense variation Q705K in CIAS1/NALP3/NLRP3 gene and an NLRP1 haplotype are associated with celiac disease. The American journal of gastroenterology. 2011; 106:539–544. [PubMed: 21245836]
21. Cummings JR, Cooney RM, Clarke G, Beckly J, Geremia A, Pathan S, Hancock L, Guo C, Cardon LR, Jewell DP. The genetics of NOD-like receptors in Crohn's disease. Tissue antigens. 2010; 76:48–56. [PubMed: 20403135]
22. De Iudicibus S, Stocco G, Martelossi S, Londero M, Ebner E, Pontillo A, Lionetti P, Barabino A, Bartoli F, Ventura A, Decorti G. Genetic predictors of glucocorticoid response in pediatric patients with inflammatory bowel diseases. J Clin Gastroenterol. 2011; 45:e1–7. [PubMed: 20697295]
23. Faustin B, Lartigue L, Bruey JM, Luciano F, Sergienko E, Bailly-Maitre B, Volkmann N, Hanein D, Rouiller I, Reed JC. Reconstituted NALP1 inflammasome reveals two-step mechanism of caspase-1 activation. Molecular cell. 2007; 25:713–724. [PubMed: 17349957]
24. Boyden ED, Dietrich WF. Nalp1b controls mouse macrophage susceptibility to anthrax lethal toxin. Nature genetics. 2006; 38:240–244. [PubMed: 16429160]

25. Kovarova M, Hesker PR, Jania L, Nguyen M, Snouwaert JN, Xiang Z, Lommatzsch SE, Huang MT, Ting JP, Koller BH. NLRP1-dependent pyroptosis leads to acute lung injury and morbidity in mice. J Immunol. 2012; 189:2006–2016. [PubMed: 22753929]

26. Witola WH, Mui E, Hargrave A, Liu S, Hypolite M, Montpetit A, Cavailles P, Bisanz C, Cesbron-Delauw MF, Fournie GJ, McLeod R. NALP1 influences susceptibility to human congenital toxoplasmosis, proinflammatory cytokine response, and fate of Toxoplasma gondii-infected monocytic cells. Infection and immunity. 2011; 79:756–766. [PubMed: 21098108]

27. Cirelli KM, Gorfu G, Hassan MA, Printz M, Crown D, Leppla SH, Grigg ME, Saeij JP, Moayeri M. Inflammasome sensor NLRP1 controls rat macrophage susceptibility to Toxoplasma gondii. PLoS pathogens. 2014; 10:e1003927. [PubMed: 24626226]

28. Ewald SE, Chavarria-Smith J, Boothroyd JC. NLRP1 is an inflammasome sensor for Toxoplasma gondii. Infection and immunity. 2014; 82:460–468. [PubMed: 24218483]

29. Masters SL, Gerlic M, Metcalf D, Preston S, Pellegrini M, O'Donnell JA, McArthur K, Baldwin TM, Chevrier S, Nowell CJ, Cengia LH, Henley KJ, Collinge JE, Kastner DL, Feigenbaum L, Hilton DJ, Alexander WS, Kile BT, Croker BA. NLRP1 inflammasome activation induces pyroptosis of hematopoietic progenitor cells. Immunity. 2012; 37:1009–1023. [PubMed: 23219391]

30. Chavarria-Smith J, Vance RE. Direct proteolytic cleavage of NLRP1B is necessary and sufficient for inflammasome activation by anthrax lethal factor. PLoS pathogens. 2013; 9:e1003452. [PubMed: 23818853]

31. Gorfu G, Cirelli KM, Melo MB, Mayer-Barber K, Crown D, Koller BH, Masters S, Sher A, Leppla SH, Moayeri M, Saeij JP, Grigg ME. Dual role for inflammasome sensors NLRP1 and NLRP3 in murine resistance to Toxoplasma gondii. mBio. 2014:5.

32. Mariathasan S, Newton K, Monack DM, Vucic D, French DM, Lee WP, Roose-Girma M, Erickson S, Dixit VM. Differential activation of the inflammasome by caspase-1 adaptors ASC and Ipaf. Nature. 2004; 430:213–218. [PubMed: 15190255]

33. Wirtz S, Neufert C, Weigmann B, Neurath MF. Chemically induced mouse models of intestinal inflammation. Nature protocols. 2007; 2:541–546.

34. Neufert C, Becker C, Neurath MF. An inducible mouse model of colon carcinogenesis for the analysis of sporadic and inflammation-driven tumor progression. Nature protocols. 2007; 2:1998–2004.

35. Allen IC, Wilson JE, Schneider M, Lich JD, Roberts RA, Arthur JC, Woodford RM, Davis BK, Uronis JM, Herfarth HH, Jobin C, Rogers AB, Ting JP. NLRP12 suppresses colon inflammation and tumorigenesis through the negative regulation of noncanonical NF-kappaB signaling. Immunity. 2012; 36:742–754. [PubMed: 22503542]

36. Meira LB, Bugni JM, Green SL, Lee CW, Pang B, Borenshtein D, Rickman BH, Rogers AB, Moroski-Erkul CA, McFaline JL, Schauer DB, Dedon PC, Fox JG, Samson LD. DNA damage induced by chronic inflammation contributes to colon carcinogenesis in mice. The Journal of clinical investigation. 2008; 118:2516–2525. [PubMed: 18521188]

37. Allen IC, Jania CM, Wilson JE, Tekeppe EM, Hua X, Brickey WJ, Kwan M, Koller BH, Tilley SL, Ting JP. Analysis of NLRP3 in the development of allergic airway disease in mice. Journal of immunology. 2012; 188:2884–2893.

38. Cressman VL, Hicks EM, Funkhouser WK, Backlund DC, Koller BH. The relationship of chronic mucin secretion to airway disease in normal and CFTR-deficient mice. American journal of respiratory cell and molecular biology. 1998; 19:853–866. [PubMed: 9843919]

39. Greten FR, Eckmann L, Greten TF, Park JM, Li ZW, Egan LJ, Kagnoff MF, Karin M. IKKbeta links inflammation and tumorigenesis in a mouse model of colitis-associated cancer. Cell. 2004; 118:285–296. [PubMed: 15294155]

40. Holl EK. Generation of bone marrow and fetal liver chimeric mice. Methods in molecular biology. 2013; 1032:315–321. [PubMed: 23943463]

41. Kupershmidt I, Su QJ, Grewal A, Sundaresh S, Halperin I, Flynn J, Shekar M, Wang H, Park J, Cui W, Wall GD, Wisotzkey R, Alag S, Akhtari S, Ronaghi M. Ontology-based meta-analysis of global collections of high-throughput public data. PloS one. 2010; 5

42. Wlodarska M, Thaiss CA, Nowarski R, Henao-Mejia J, Zhang JP, Brown EM, Frankel G, Levy M, Katz MN, Philbrick WM, Elinav E, Finlay BB, Flavell RA. NLRP6 inflammasome orchestrates the colonic host-microbial interface by regulating goblet cell mucus secretion. Cell. 2014; 156:1045–1059. [PubMed: 24581500]
43. Su L, Shen L, Clayburgh DR, Nalle SC, Sullivan EA, Meddings JB, Abraham C, Turner JR. Targeted epithelial tight junction dysfunction causes immune activation and contributes to development of experimental colitis. Gastroenterology. 2009; 136:551–563. [PubMed: 19027740]
44. Carvalho FA, Nalbantoglu I, Aitken JD, Uchiyama R, Su Y, Doho GH, Vijay-Kumar M, Gewirtz AT. Cytosolic flagellin receptor NLRC4 protects mice against mucosal and systemic challenges. Mucosal immunology. 2012; 5:288–298. [PubMed: 22318495]
45. Satsangi J, Wolstencroft RA, Cason J, Ainley CC, Dumonde DC, Thompson RP. Interleukin 1 in Crohn's disease. Clinical and experimental immunology. 1987; 67:594–605. [PubMed: 3496997]
46. Reinecker HC, Steffen M, Witthoeft T, Pflueger I, Schreiber S, MacDermott RP, Raedler A. Enhanced secretion of tumour necrosis factor-alpha, IL-6, and IL-1 beta by isolated lamina propria mononuclear cells from patients with ulcerative colitis and Crohn's disease. Clinical and experimental immunology. 1993; 94:174–181. [PubMed: 8403503]
47. McAlindon ME, Hawkey CJ, Mahida YR. Expression of interleukin 1 beta and interleukin 1 beta converting enzyme by intestinal macrophages in health and inflammatory bowel disease. Gut. 1998; 42:214–219. [PubMed: 9536946]
48. Ben-Sasson SZ, Hu-Li J, Quiel J, Cauchetaux S, Ratner M, Shapira I, Dinarello CA, Paul WE. IL-1 acts directly on CD4 T cells to enhance their antigen-driven expansion and differentiation. Proceedings of the National Academy of Sciences of the United States of America. 2009; 106:7119–7124. [PubMed: 19359475]
49. Sutton CE, Lalor SJ, Sweeney CM, Brereton CF, Lavelle EC, Mills KH. Interleukin-1 and IL-23 induce innate IL-17 production from gammadelta T cells, amplifying Th17 responses and autoimmunity. Immunity. 2009; 31:331–341. [PubMed: 19682929]
50. Acosta-Rodriguez EV, Napolitani G, Lanzavecchia A, Sallusto F. Interleukins 1beta and 6 but not transforming growth factor-beta are essential for the differentiation of interleukin 17-producing human T helper cells. Nature immunology. 2007; 8:942–949. [PubMed: 17676045]
51. Chung Y, Chang SH, Martinez GJ, Yang XO, Nurieva R, Kang HS, Ma L, Watowich SS, Jetten AM, Tian Q, Dong C. Critical regulation of early Th17 cell differentiation by interleukin-1 signaling. Immunity. 2009; 30:576–587. [PubMed: 19362022]
52. Coccia M, Harrison OJ, Schiering C, Asquith MJ, Becher B, Powrie F, Maloy KJ. IL-1beta mediates chronic intestinal inflammation by promoting the accumulation of IL-17A secreting innate lymphoid cells and CD4(+) Th17 cells. The Journal of experimental medicine. 2012; 209:1595–1609. [PubMed: 22891275]
53. Carbo A, Hontecillas R, Kronsteiner B, Viladomiu M, Pedragosa M, Lu P, Philipson CW, Hoops S, Marathe M, Eubank S, Bisset K, Wendelsdorf K, Jarrah A, Mei Y, Bassaganya-Riera J. Systems modeling of molecular mechanisms controlling cytokine-driven CD4+ T cell differentiation and phenotype plasticity. Plos Comput Biol. 2013; 9:e1003027. [PubMed: 23592971]
54. Leach ST, Messina I, Lemberg DA, Novick D, Rubenstein M, Day AS. Local and systemic interleukin-18 and interleukin-18-binding protein in children with inflammatory bowel disease. Inflammatory bowel diseases. 2008; 14:68–74. [PubMed: 17879274]
55. Ben Aleya W, Sfar I, Habibi I, Mouelhi L, Aouadi H, Makhlouf M, Ayed-Jendoubi S, Najjar T, Ben Abdallah T, Ayed K, Gorgi Y. Interleukin-18 gene polymorphisms in tunisian patients with inflammatory bowel disease. Digestion. 2011; 83:269–274. [PubMed: 21273776]
56. Sivakumar PV, Westrich GM, Kanaly S, Garka K, Born TL, Derry JM, Viney JL. Interleukin 18 is a primary mediator of the inflammation associated with dextran sulphate sodium induced colitis: blocking interleukin 18 attenuates intestinal damage. Gut. 2002; 50:812–820. [PubMed: 12010883]
57. Araki A, Kanai T, Ishikura T, Makita S, Uraushihara K, Iiyama R, Totsuka T, Takeda K, Akira S, Watanabe M. MyD88-deficient mice develop severe intestinal inflammation in dextran sodium sulfate colitis. Journal of gastroenterology. 2005; 40:16–23. [PubMed: 15692785]

58. Salcedo R, Worschech A, Cardone M, Jones Y, Gyulai Z, Dai RM, Wang E, Ma W, Haines D, O'HUigin C, Marincola FM, Trinchieri G. MyD88-mediated signaling prevents development of adenocarcinomas of the colon: role of interleukin 18. The Journal of experimental medicine. 2010; 207:1625–1636. [PubMed: 20624890]

59. Bersudsky M, Luski L, Fishman D, White RM, Ziv-Sokolovskaya N, Dotan S, Rider P, Kaplanov I, Aychek T, Dinarello CA, Apte RN, Voronov E. Non-redundant properties of IL-1alpha and IL-1beta during acute colon inflammation in mice. Gut. 2014; 63:598–609. [PubMed: 23793223]

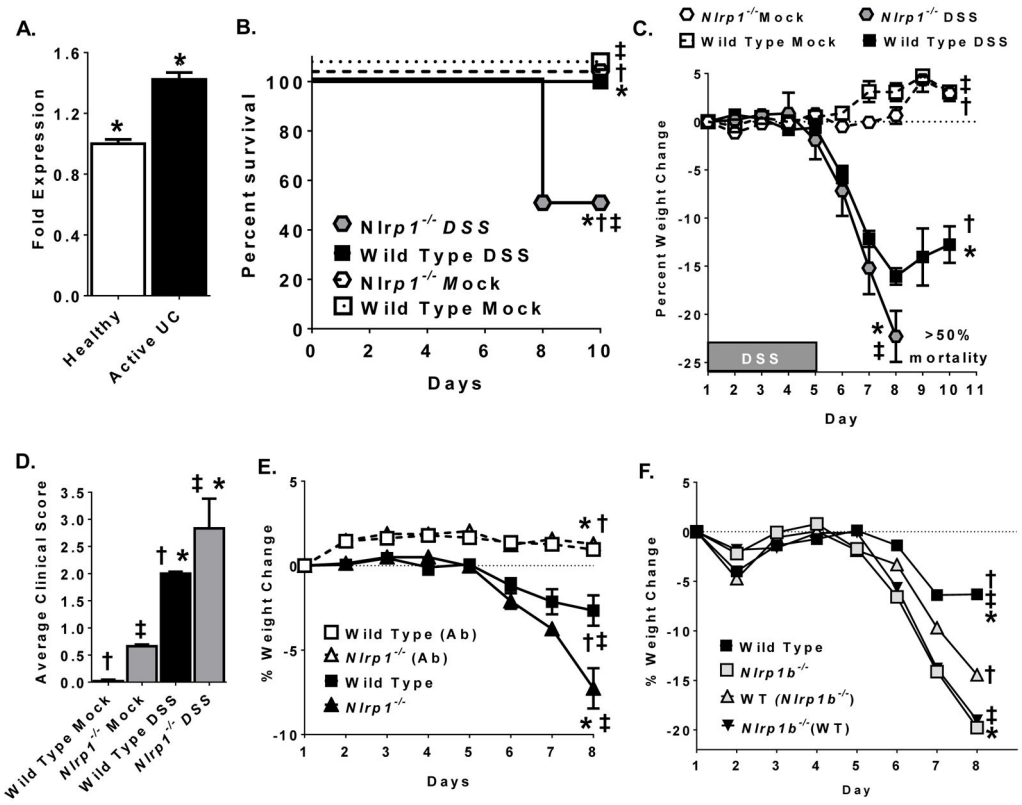

Figure 1. NLRP1 dysregulation is associated with ulcerative colitis

A. Retrospective analysis of metadata from colonic biopsies collected from UC patients revealed that *NLRP1* expression was significantly up-regulated. The fold-change values were averaged from 3 separate datasets and reflect the change in the expression between the affected tissues of UC patients with active disease compared to healthy controls. *p<0.01. **B.** Kaplan-Meier plot of *Nlrp1b*$^{-/-}$ and wild type mouse survival. *Nlrp1b*$^{-/-}$ animals were euthanized on day 8 due to increased weight loss and clinical parameters associated with disease progression. *p<0.01; †p<0.01; ‡ p<0.01. **C.** *Nlrp1b*$^{-/-}$ mice exhibited significant weight loss following DSS exposure compared to the wild type animals. *p<0.05; †p<0.01; ‡ p<0.01. **D.** *Nlrp1b*$^{-/-}$ mice exhibit enhanced clinical parameters associated with disease progression, including increased weight loss, stool consistency, and bleeding, compared to the wild type animals. *p<0.05; †p<0.01; ‡ p<0.01. Wild Type Mock, n=3; Wild Type DSS, n=5; *Nlrp1b*$^{-/-}$ Mock, n=5; *Nlrp1b*$^{-/-}$ DSS, n=6. **E.** *Nlrp1b*$^{-/-}$ mice and wild type animals were treated with an antibiotic cocktail throughout the duration of DSS exposure (2.5% DSS) and disease progression was evaluated. *p<0.01; †p<0.01; ‡p<0.01. Wild Type DSS, n=5; Wild Type DSS+Antibiotic (Ab), n=15; *Nlrp1b*$^{-/-}$ DSS, n=5; *Nlrp1b*$^{-/-}$ DSS+Ab, n=15. **F.** *Nlrp1b*$^{-/-}$ mice and wild type (WT) animals were weaned and cohoused in a 1:1 ratio for 8 weeks prior to DSS exposure. Wild Type DSS, n=3; *Nlrp1b*$^{-/-}$, n=3; Wild Type mice co-housed with *Nlrp1b*$^{-/-}$ (WT(*Nlrp1b*$^{-/-}$)), n=10; *Nlrp1b*$^{-/-}$ mice cohoused with wild type (*Nlrp1b*$^{-/-}$(WT)), n=10. *p<0.01; †p<0.05; ‡p<0.01. Data are representative of greater than 3 independent experiments.

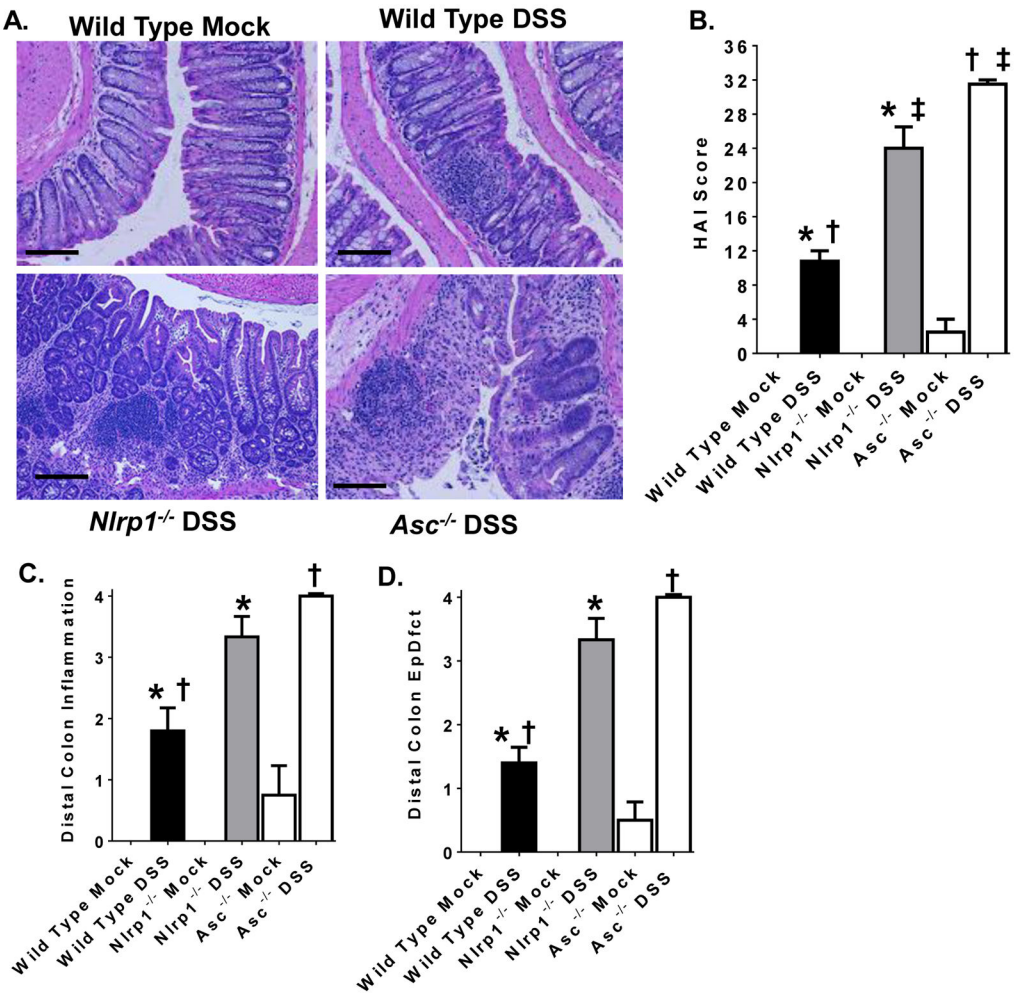

Figure 2. The NLRP1 inflammasome attenuates gastrointestinal inflammation during experimental colitis progression

A. Increased inflammation and epithelial cell damage was observed in the colons of all DSS treated animals following H&E staining. Increased disease histopathology was observed in *Nlrp1b*$^{-/-}$ mice compared to wild type animals; however, *Asc*$^{-/-}$ mice demonstrated the most severe features of disease pathogenesis. Scale bar: 250μm. **B.** The Histologic Activity Index (HAI) Score was determined from colon sections collected from *Nlrp1b*$^{-/-}$, *Asc*$^{-/-}$ and wild type mice. *p<0.05; †p<0.05; ‡p<0.05. **C–D.** Distal colon inflammation and epithelial cell defects were significantly increased components of the HAI score for both *Nlrp1b*$^{-/-}$ and *Asc*$^{-/-}$ animals compared to the wild type mice. *p<0.05; †p<0.05. Wild Type Mock, n=3; Wild Type DSS, n=5; *Nlrp1b*$^{-/-}$ Mock, n=5; *Nlrp1b*$^{-/-}$ DSS, n=6; *Asc*$^{-/-}$ Mock, n=5; *Asc*$^{-/-}$ DSS, n=6. Data shown were generated from colon sections collected from mice on Day 8 and are representative of more than 5 independent experiments.

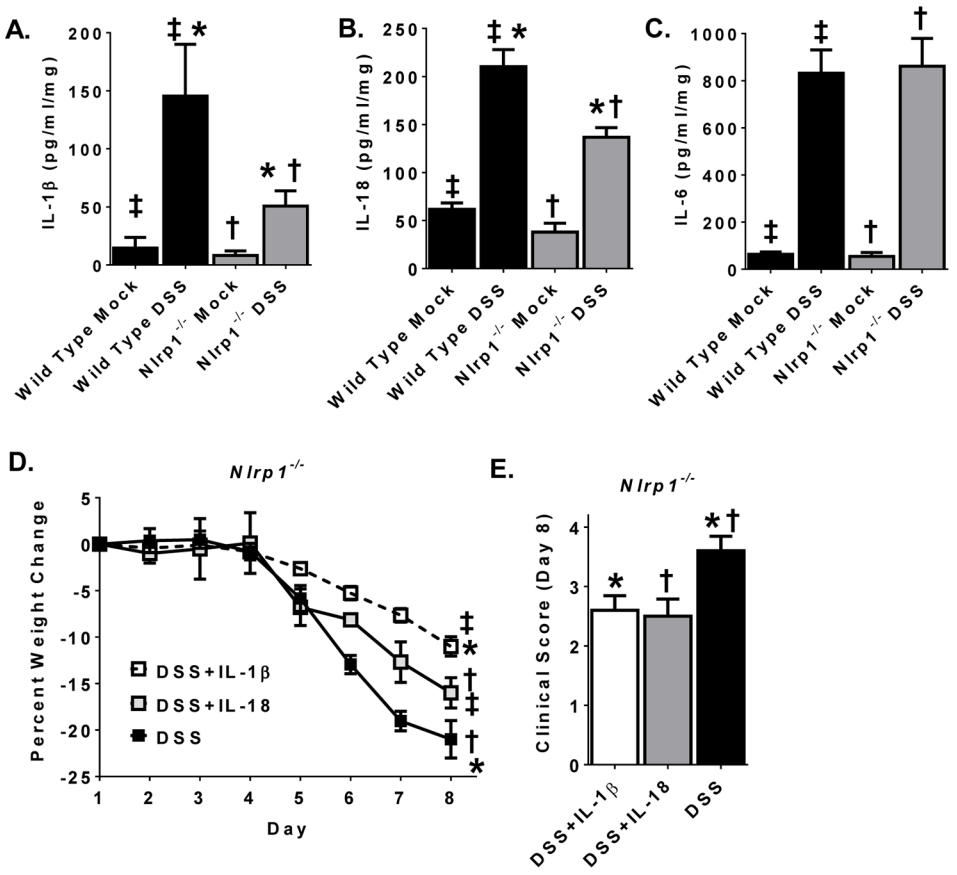

Figure 3. NLRP1 regulates IL-1β and IL-18 levels in the colon during experimental colitis

A–C. Colon sections were isolated, weighed and cultured overnight from wild type and *Nlrp1b*$^{-/-}$ mice following treatment with DSS (Day 8). Secreted cytokine levels were evaluated in cell free supernatants using ELISA. **A.** IL-1β levels were significantly increased in all of the organ culture supernatants collected from DSS exposed animals. However, IL-1β was significantly reduced in the *Nlrp1b*$^{-/-}$ mice compared to the wild type animals. *p<0.05; †p<0.05; ‡p<0.05. **B.** IL-18 levels were significantly attenuated in the organ culture supernatants from the *Nlrp1b*$^{-/-}$ mice compared to the wild type animals. *p<0.05; †p<0.01; ‡p<0.01. **C.** IL-6 levels were significantly increased in both wild type and *Nlrp1b*$^{-/-}$ animals following DSS exposure, with no differences between genotypes. †p<0.01; ‡p<0.01. Wild Type Mock, n=3; Wild Type DSS, n=5; *Nlrp1b*$^{-/-}$ Mock, n=5; *Nlrp1b*$^{-/-}$ DSS, n=6; *Asc*$^{-/-}$ Mock, n=5; *Asc*$^{-/-}$ DSS, n=6. **D–E**. *Nlrp1b*$^{-/-}$ mice were injected i.p. with either recombinant mouse IL-1β or IL-18 daily during DSS exposure. Reconstitution with either IL-1β or IL-18 significantly improved both weight loss and clinical score. DSS only, n=5; DSS+IL-1β, n=5; DSS+IL-18, n=4. *p<0.01; †p<0.05; ‡p<0.05. Data are representative of more than 3 independent experiments.

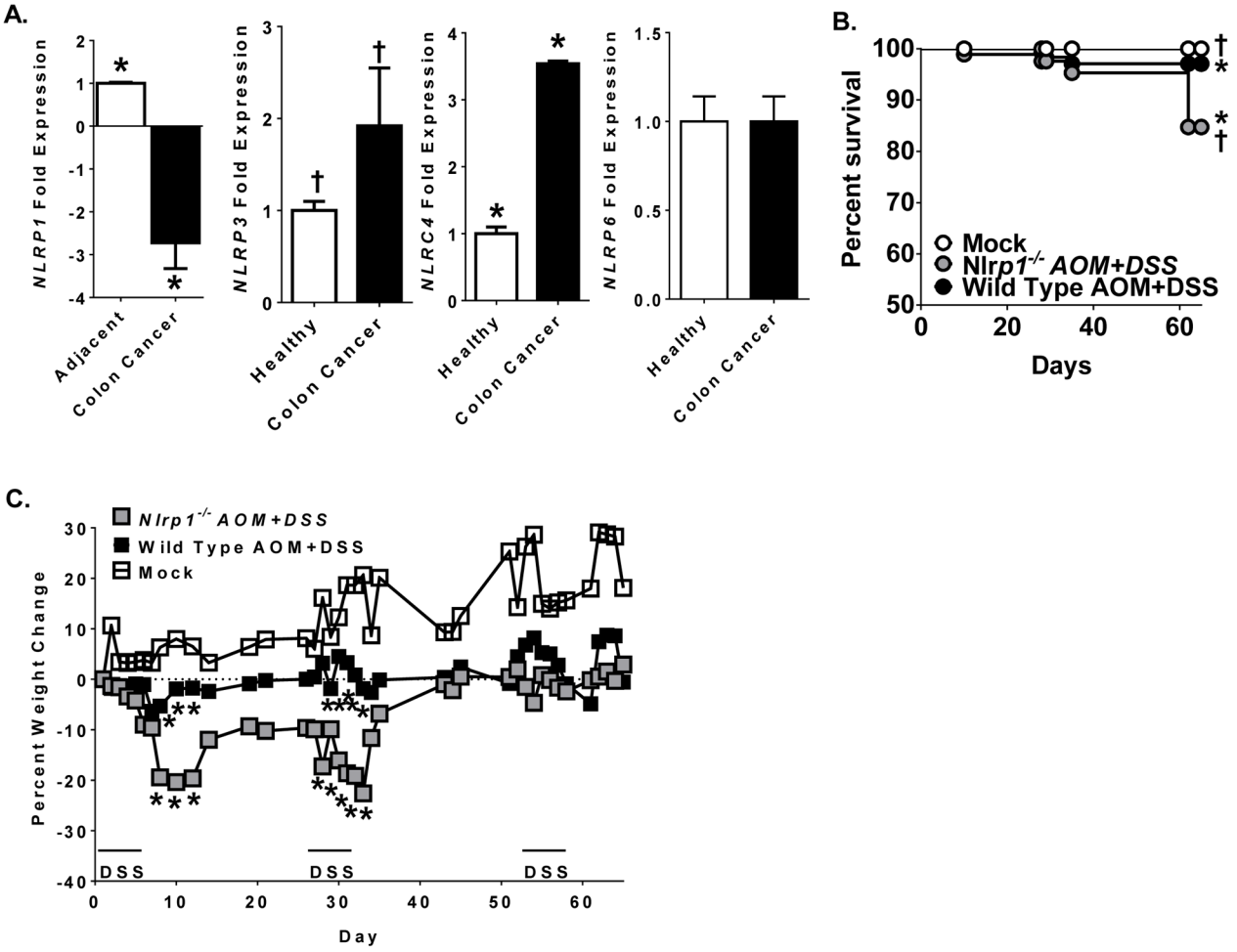

Figure 4. NLRP1 attenuates the progression of colitis associated tumorigenesis

A. Retrospective analysis of metadata from colonic biopsies collected from CRC patients. Expression of NLRP1 and other NLRs previously associated with cancer were evaluated. Expression of each NLR was assessed from biopsies collected from polyps or characterized adenocarcinomas and compared with either adjacent polyp free areas of the colon or from biopsies collected from healthy control subjects as indicated. The fold-change values were averaged from 5 separate datasets. *p<0.001; †p<0.01. **B–C**. *Nlrp1b*$^{-/-}$ mice were hypersensitive to the AOM/DSS inflammation driven colon tumorigenesis model. **B.** Kaplan-Meier plot of *Nlrp1b*$^{-/-}$ and wild type mouse survival. *p<0.05; †p<0.05. **C**. *Nlrp1b*$^{-/-}$ mice demonstrated significant weight loss throughout the majority of the AOM/DSS model compared to wild type animals. *p<0.05. Wild Type Mock, n=3; Wild Type AOM, n=3; Wild Type DSS, n=5; Wild Type AOM/DSS, n=12; *Nlrp1b*$^{-/-}$ Mock, n=3; *Nlrp1b*$^{-/-}$ AOM, n=3; *Nlrp1b*$^{-/-}$ DSS, n=6; *Nlrp1b*$^{-/-}$ AOM/DSS, n=9. Data are representative of 3 independent experiments.

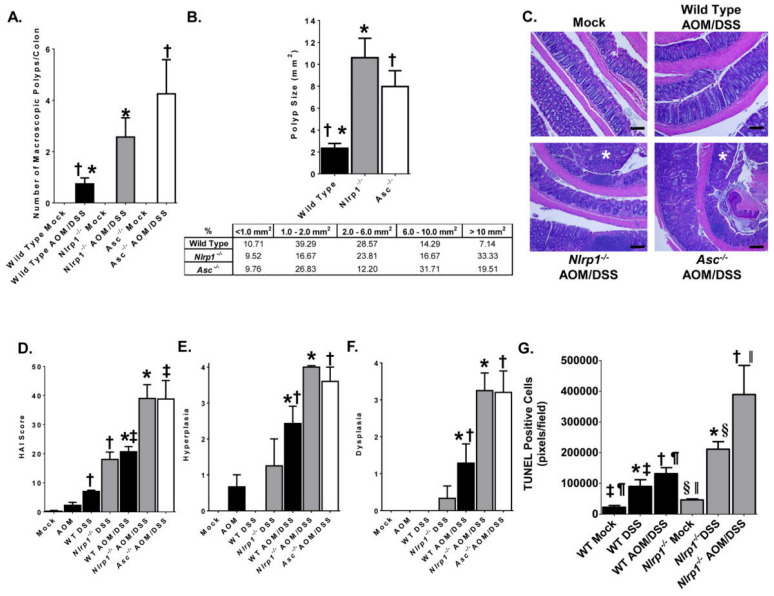

%	<1.0 mm²	1.0 - 2.0 mm²	2.0 - 6.0 mm²	6.0 - 10.0 mm²	> 10 mm²
Wild Type	10.71	39.29	28.57	14.29	7.14
Nlrp1$^{-/-}$	9.52	16.67	23.81	16.67	33.33
Asc$^{-/-}$	9.76	26.83	12.20	31.71	19.51

Figure 5. The NLRP1 inflammasome attenuates tumorigenesis during colitis associated cancer

A. The number of macroscopic polyps were determined in *Nlrp1b*$^{-/-}$, *Asc*$^{-/-}$ and wild type colons upon necropsy following the completion of the CAC model. *p<0.05; †p<0.05. **B.** The maximal cross-sectional area of macroscopic polyps was determined for each genotype. The percent of polyps per size range is shown in the table *p<0.01; †p<0.01. **C.** Representative histopathology illustrating increased inflammation, hyperplasia and dysplasia in the *Nlrp1b*$^{-/-}$ and *Asc*$^{-/-}$ mice compared to the wild type animals. Areas of neoplasia in the *Nlrp1b*$^{-/-}$ and *Asc*$^{-/-}$ colons are denoted with an *. Scale bar: 250μm. **D.** The composite HAI score was calculated for each set of experimental groups evaluated upon completion of the CAC model. *p<0.05; †p<0.05; ‡p<0.05. **E–F.** Histopathology analysis revealed increased colon hyperplasia and dysplasia in all of the animals treated with AOM/DSS. However, a significant increase was observed in both parameters in colons evaluated from the *Nlrp1b*$^{-/-}$ and *Asc*$^{-/-}$ mice. *p<0.05; †p<0.05. **G.** TUNEL staining of histopathology sections revealed a significant increase in TUNEL positive cells following either DSS or AOM/DSS exposure. Computer assisted image analysis revealed a significant increase in TUNEL positive cells in *Nrlp1b*$^{-/-}$ mice in both models compared to wild type animals. *p<0.05; †p<0.05; ‡p<0.01; §p<0.01; ¶p<0.01; ||p<0.01. Wild Type Mock, n=3; Wild Type AOM, n=3; Wild Type DSS, n=5; Wild Type AOM/DSS, n=12; *Nlrp1b*$^{-/-}$ Mock, n=3; *Nlrp1b*$^{-/-}$ AOM, n=3; *Nlrp1b*$^{-/-}$ DSS, n=6; *Nlrp1b*$^{-/-}$ AOM/DSS, n=9; *Asc*$^{-/-}$ mock, n=3; *Asc*$^{-/-}$ AOM/DSS, n=8. All studies were evaluated on Day 64. Data are representative of 3 independent experiments.

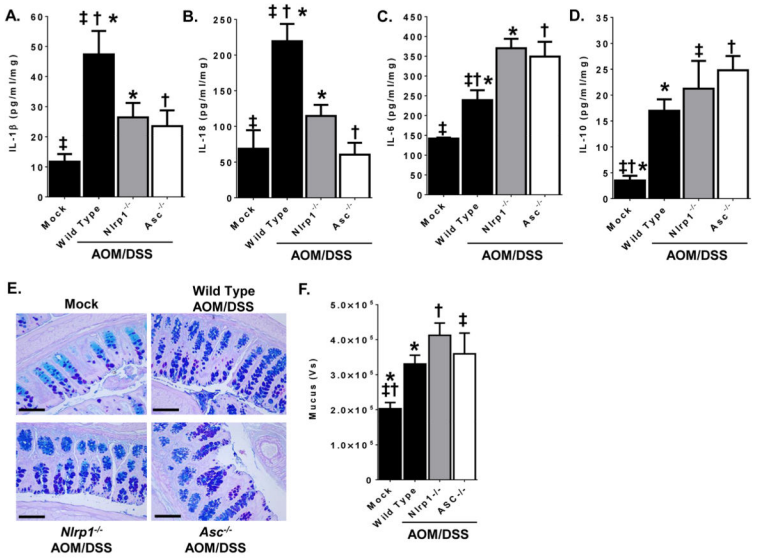

Figure 6. The NLRP1 inflammasome modulates IL-1β and IL-18 levels during colitis associated tumorigenesis

A–B. Colon IL-1β and IL-18 levels were significantly reduced in the *Nlrp1b*$^{-/-}$ and *Asc*$^{-/-}$ mice compared to the wild type animals. *p<0.05; †p<0.05; ‡p<0.01. **C.** IL-6 levels were increased in the colons harvested from all animals treated with AOM/DSS and were significantly increased in the colons collected from the *Nlrp1b*$^{-/-}$ and *Asc*$^{-/-}$ animals compared to the wild type tissues. *p<0.05; †p<0.05; ‡p<0.05. **D.** IL-10 was significantly up-regulated in the colon tissue following induction of colitis associated tumorigenesis; however, no significant differences were observed between genotypes. *p<0.01; †p<0.01; ‡p<0.05. **E.** Mucus production in the colon was evaluated by AB/PAS staining. Representative histopathology illustrating increased goblet cell hyperplasia (AB/PAS+ staining) and mucus production in all of the AOM/DSS treated animals. Scale bar: 250μm. **F.** AB/PAS+ staining was quantified utilizing imaging analysis software (ImageJ) along a 2 mm section of the colon, located approximately 1 cm proximal from the termination of the rectum. Data are represented as Vs. *p<0.05; †p<0.05; ‡p<0.05. Wild Type Mock, n=3; Wild Type AOM/DSS, n=12; *Nlrp1b*$^{-/-}$ Mock, n=3 (not shown); *Nlrp1b*$^{-/-}$ AOM/DSS, n=9; *Asc*$^{-/-}$ Mock, n=3 (not shown); *Asc*$^{-/-}$ AOM/DSS, n=8. Data shown were generated from colon sections collected from mice on Day 64 and are representative of 5 independent experiments.

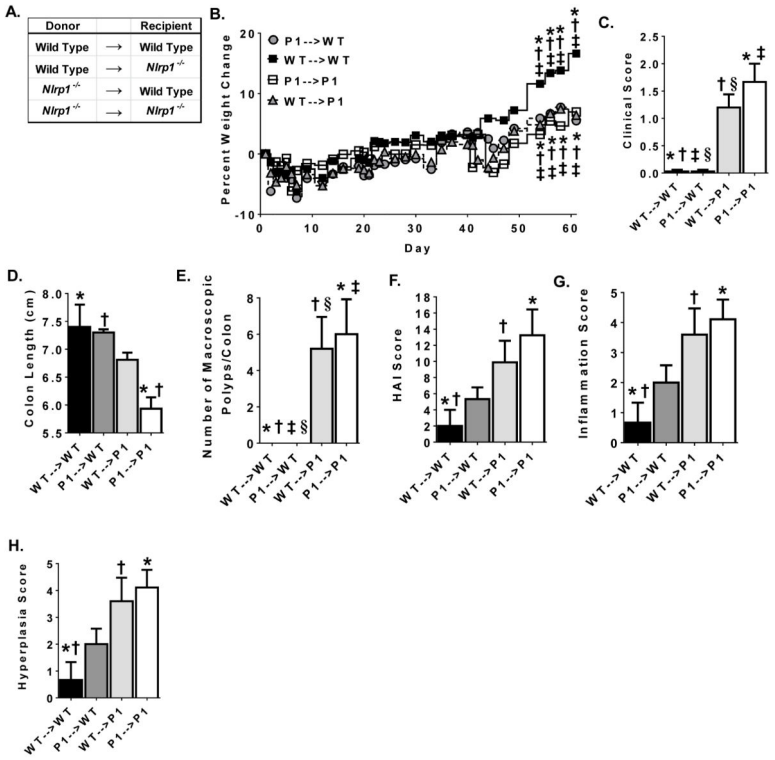

Figure 7. NLRP1 attenuates colitis associated tumorigenesis through non-hematopoietic derived cells

A. Schematic of bone marrow chimera mice. **B.** Weight change of each chimeric mouse group revealed that all of the chimeric mice demonstrated a significant reduction in weight loss compared to the wild type→wild type (WT→WT) mice. *Nlrp1b*$^{-/-}$→*Nlrp1b*$^{-/-}$ (P1→P1) *p<0.05; *Nlrp1b*$^{-/-}$→WT (P1→WT) †p<0.05; WT→*Nlrp1b*$^{-/-}$ (WT→P1) ‡p<0.05. **C.** Scoring associated with clinical disease parameters revealed that WT→*Nlrp1b*$^{-/-}$ mice phenocopied the *Nlrp1b*$^{-/-}$→*Nlrp1b*$^{-/-}$ animals; whereas, no difference was observed between the *Nlrp1b*$^{-/-}$→WT and WT→WT animals. *p<0.01; †p<0.01; ‡p<0.01; §p<0.01**. D.** Colons from the *Nlrp1b*$^{-/-}$→*Nlrp1b*$^{-/-}$ animals were significantly truncated compared to the *Nlrp1b*$^{-/-}$→WT and WT→WT animals, while the colons from the WT→*Nlrp1b*$^{-/-}$ mice were an intermediate length. *p<0.01; †p<0.01**. E.** The number of macroscopic polyps were determined in colons from the chimeric mice upon necropsy following the completion of the CAC model. *p<0.01; †p<0.01; ‡p<0.01; §p<0.01**. F.** The composite HAI score was calculated for each set of experimental groups evaluated upon completion of the CAC model. *p<0.05; †p<0.05. **G–H.** Histopathology analysis revealed increased **(G)** inflammation and **(H)** hyperplasia in both the proximal and distal colon in the WT→*Nlrp1b*$^{-/-}$ and *Nlrp1b*$^{-/-}$→*Nlrp1b*$^{-/-}$ animals compared to the WT→WT mice. WT→WT, n=4; WT→*Nlrp1b*$^{-/-}$, n=9; *Nlrp1b*$^{-/-}$→WT, n=4; *Nlrp1b*$^{-/-}$→*Nlrp1b*$^{-/-}$, n=6. Female mice were used in the chimera studies. Data shown are representative of 2 independent experiments.